Periodica Polytechnica
Mechanical Engineering

CFD Analysis of Double Suction Centrifugal Pump with Double Volute

62(1), pp. 74-82, 2018
https://doi.org/10.3311/PPme.11425

Pranav Vyavahare[1], Lokavarapu Bhaskara Rao[1*], Nilesh Patil[2]

RESEARCH ARTICLE

Received 26 August 2017; accepted after revision 05 December 2017

Abstract

In this study, Computational Fluid Dynamics (CFD) Analysis is used to investigate the flow in the centrifugal pump impeller using the ANSYS-CFX. Impeller is designed for head of 22 m, discharge of 52.239 m³/hr and for the operating speed of 2970 RPM. Impeller vane profile is generated by tangent arc method and CFD analysis is performed for 1st stage of vertical pump out of 15 stages. Velocity and pressure distribution are analysed for casing and impeller. Using ANSYS-CFX head developed by this impeller is calculated and compared with the required value. From results of CFD analysis, performance curves are plotted and compared with analytical performance curves. Results obtained from CFD nearly matches with analytical results.

Keywords

CFD, vertical pump, head, impeller, volute casing

[1] School of Mechanical and Building Sciences, VIT Chennai, Vandalur-Kelambakkam Road, Chennai-600127, Tamil Nadu, India

[2] Design Engineering Division, KEPL, Kirlosakarwadi, Maharashtra- 416308, Indi, India

[*] Corresponding author, e-mail: bhaskarbabu_20@yahoo.com

1 Introduction

Pump is designed as per API 610 standards. Modelling of impeller, volute geometry and all pump components is done in software CREO 3.0 by assuming the required duty parameters. Double suction impeller is designed to meet required head and flow at operating speed. Double volute casing is used to transfer fluid from inlet to outlet pipe.

Nowadays the use of CFD plays an important role in fluid mechanics. Due to the progress in computer capability and numerical methods, the design analysis of centrifugal pumps by using 3D-Navier stokes program or CFD software has become easy. The impeller could be redesigned if the final result from the CFD differs from the designed value [1].

Number of researchers has studied the application of CFD in fluid mechanics and turbo machinery over the years [1-7]. However, there are few researchers used this CFD tool to predict the performance of pump impeller. Until now, there have been only three works carried out by Rajendran and Purushothaman [8], Damor et al. [9], Patel and Patel [10] in dealing with this issue.

For a standard k-ε turbulence model Rajendran and Purushothaman [8] used a commercial 3D-Navier Stokes program. The stream line pattern, pressure contours on a blade surface, blade forces and pressure plots are discussed in this paper. Experimental Investigations on centrifugal water pump is conducted by Damor et al. [9] with outlet impeller diameter of 111-mm, backward curved blades, 4.0 liters per second of nominal discharge and 12 m of head to assess the effect of various operating conditions like power, speed, discharge and head on the performance of the pump. Patel and Patel [10] performed CFD analysis of enclosed impeller at various inlet and outlet blade angles of the impeller and number of blades of impeller and investigated the changes in head as well as efficiencies. Zhou et al., [11] described the three-dimensional simulation of internal flow in three different types of centrifugal pumps. Maitelli et al., [12] presented a 3D simulation of the stationary flow in the impeller and stator of a mixed centrifugal pump using CFD techniques. Three conditions were simulated to obtain the pressure fields in the impeller and stator in a stage of the pump. Ajith and Jeoju [13] generated impeller vane profile by

circular arc method and point by point method and performed CFD analysis for the impeller vane profile. Further the impeller was analyzed for both forward and backward curved vane. Rajiv Kaul [14] carried out the design and numerical analysis of Centrifugal pump. A design of Centrifugal pump is carried out and numerically analyzed to get the best performance point. Tilahun Nigussie and Edessa Dribssa [15] determined the pattern of velocity profile and pressure distribution by using CFD simulation program after the 3D design and modeling of the pump is made using Vista CPD.

Although some data is at present accessible on applying the CFD for anticipating of radial flow type impeller, for detailed research there still remains room. In the present study, the main concern is to predict head developed by impeller at any volumetric flow rate and compare with theoretical value, compare efficiency of impeller at various volumetric flow rates, elucidate the method to validate the CFD results. Secondary objective is to plot the velocity and pressure distribution plots to ensure the laminar flow at outlet.

2 Design of impeller

Double suction impeller is used in this study to generate required head. For designing impeller following parameters are considered as input,

$$\text{Head} = 22\text{m}.$$

$$\text{Flowrate} = 52.239\,\text{m}^3/\text{sec} = \frac{52.239}{3600}$$

$$\text{Flowrate} = 0.01451\,\text{m}^3/\text{sec}.$$

But impeller is double suction, hence

$$Q = \frac{0.01451}{2} = 0.007255\,\text{m}^3/\text{sec}.$$

Motor Speed = 2970 rpm.
Impeller eye diameter = 84 mm

2.1 Suction velocity

The velocity of liquid at suction flange is calculated from Eq. (1)

$$Q = \text{Area} \times \text{Velocity}. \tag{1}$$

Consider maximum leakage is 2% in case of double suction impeller, the discharge is calculated from Eq. (2),

$$Q_n = 1.02\ \ Q = AV_o. \tag{2}$$

$$1.02 * 0.007255 = \frac{\pi}{4}\left(D_o^2 - D_H^2\right) * V_o$$

$$1.02 \times 0.007255 = \frac{\pi}{4}\left(0.06880^2 - 0.0381^2\right) * V_o$$

$$V_0 = 2.8709\,\text{m}^3/\text{sec}.$$

Therefore, the velocity at suction flange is 2.8709 m/sec.

2.2 Impeller inlet dimensions and angle

The inlet diameter = Eye diameter (D1) = 84 mm.

Fig. 1 shows the inlet velocity triangle. Therefore, tangential velocity of inlet vane edge is given by Eq. (3),

$$u_1 = \omega \times r_1 = \frac{2\pi ND_1}{60 \times 2} = \frac{2\pi \times 2970 \times 0.084}{60 \times 2}$$
$$u_1 = 13.062\,\text{m/sec}. \tag{3}$$

where,

V_{r1} = Radial component of inlet velocity
W_1 = Radial velocity of water at inlet
u_1 = Tangential velocity of impeller at inlet

Because converging path is more efficient than diverging path, the radial velocity should be slightly higher than V_o. So, the inlet velocity is 1.18 times that of V_o [16], now V_{r1} can be calculated from Eq. (4) as,

$$V_{r1} = 1.18 \times V0 = 1.18 \times 2.87095$$
$$V_{r1} = 3.3877\,\text{m/sec}. \tag{4}$$

The inlet vane angle can be calculated from Fig. 1 and given in Eq. (5),

$$\beta_1 = \tan^{-1}\left(\frac{V_{r1}}{u_1}\right) = \tan^{-1}\left(\frac{3.3877}{13.0627}\right)$$
$$\beta_1 = 14.53880° \tag{5}$$

To take care of the contraction of the stream as it passes the inlet edges as well as pre-rotation, β_1 is usually increased slightly. As suggested by Church [16] for better performance, the inlet angle should be between 100° to 250°. Hence taking, β_1= 220°. Therefore, V_{r1} can be calculated from Fig. 1 and given in Eq. (6),

$$V_{r1} = u_1 \tan\beta_1 = 13.0627 \tan(22)$$
$$V_{r1} = 5.2776\,\text{m/sec} \tag{6}$$

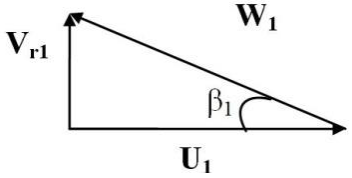

Fig. 1 Inlet velocity triangle

2.3 Impeller outer diameter D_2

The theoretical head can be found from integrating the force on a differential mass [16]. Fig. 2 represents differential mass plot,

$$dF = dmr\omega^2. \tag{7}$$

$$dP = \frac{dF}{A}. \tag{8}$$

$$dm = \rho d\forall = \rho brd\varnothing dr \tag{9}$$

From Eq. (7) to (9), we get following,

$$\int_1^2 dP = \int_1^2 \frac{\rho brd\varnothing dr.r\omega^2}{brd\varnothing} = \rho\omega^2 \int_1^2 rdr = \frac{\rho\omega^2}{2}\left(r_2^2 - r_1^2\right)$$

And

$$U = r * \omega \tag{10}$$

$$H = \frac{P}{\rho g} \tag{11}$$

From Eq. (10) and (11),

$$H_2 - H_1 = \frac{P_2 - P_1}{\rho g} \tag{12}$$

The pressure head developed at the outer rim is,

$$H_2 = \frac{U_2^2}{2g} \tag{13}$$

Substituting $D_2*\omega/2$ for U_2 and solving for D_2 in Eq. (13), gives the following,

$$D_2 = \frac{2\sqrt{2gH_2}}{\omega} \tag{14}$$

Substituting all above values in Eq. (14) gives the outside diameter of impeller,

$$D_2 = \frac{2\sqrt{2\times 9.81\times H}}{2\pi N/60} = \frac{2\times\sqrt{2\times 9.81\times 22}}{2\pi\times 2970/60} = 133.59\text{mm}$$

Hence, Impeller outside diameter is 137 mm.

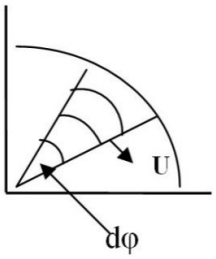

Fig. 2 Differential mass

2.4 Impeller outer dimensions and angles

Parameters of suction impeller are as shown in Fig. 3. For the better efficiency of pump, the range for outlet vane angle is 15° to 40°. Therefore, taking β_2 = 31°. But the outlet radial velocity V_{r2} is made the same as or slightly less than the radial inlet velocity V_{r1} [16]. Hence outlet velocity can be calculated as,

$$V_{r2} = 0.8 * V_{r1} = 4.2221\,\text{m/s}$$

Tangential velocity of outlet vane edge, U_2 is given by Eq. (15),

$$U_2 = \omega_{r2} = \frac{2\pi ND_2}{60*2} = \frac{2\pi X 2970 X 0.137}{120} \tag{15}$$
$$U_2 = 21.3047\,\text{m/s}$$

Fig. 4 shows the inlet and outlet velocity triangles.

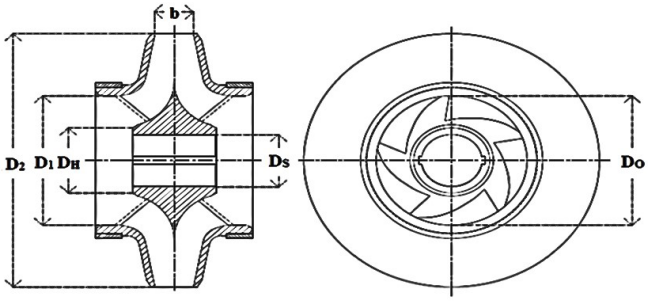

Fig. 3 Parameters of suction impeller

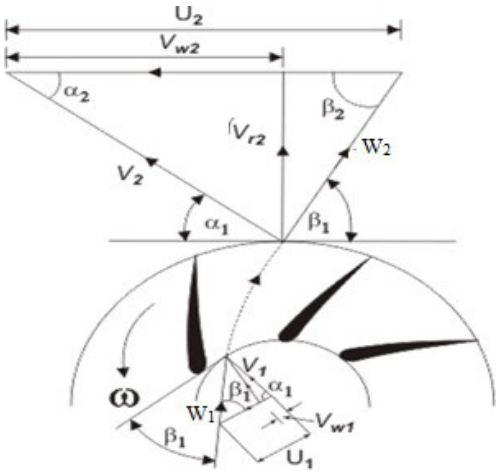

Fig. 4 Inlet and outlet velocity triangle

The number of vanes on impeller can be calculated from Eq. (16),

$$z = 6.5\left(\frac{D_2 + D_H}{D_2 - D_H}\right) * \sin\beta_m$$
$$\beta_m = \frac{\beta_1 + \beta_2}{2} = \frac{22 + 31}{2} = 26.5° \tag{16}$$

D_2 = Outside diameter of Impeller = 137 mm,
β_2 = Outlet angle = 31°
D_H = Hub diameter of Impeller = 38 mm,
β_1 = Inlet angle = 22°
Number of vanes (Z) = 5.12 so taking it as 5.

Further, theoretical tangential outlet velocity is given in Eq. (17),

$$V_{\theta 2} = U_2 - \frac{V_{r2}}{\tan\beta_2} = 21.30 - \frac{4.2221}{\tan 31°}$$
$$V_{\theta 2} = 14.0032\,\text{m/sec}. \tag{17}$$

Circular flow coefficient can be calculated using Eq. (18) [16],

$$\eta_\theta = \frac{1}{\left[1+\frac{\alpha}{z}\left(1+\frac{\beta_2}{60}\right)\left(\frac{2}{1-\left(\frac{r_1^2}{r_2^2}\right)}\right)\right]}$$

$$\eta_\theta = \frac{1}{\left[1+\frac{0.75}{6}\left(1+\frac{31}{60}\right)\left(\frac{2}{1-\left(\frac{42^2}{68.5^2}\right)}\right)\right]} \quad (18)$$

$$\eta_\theta = 0.5783$$

Therefore, actual tangential velocity at outlet is given by,

$$V'_{\theta 2} = \eta_\theta * V_{\theta 2} = 8.0980\,\text{m/sec}. \quad (19)$$

Angle of water leaving the impeller can be calculated from Eq. (20),

$$\alpha'_2 = \tan^{-1}\frac{V_{r2}}{V_{\theta 2}} = 16.7785^\circ \quad (20)$$

Absolute velocity of water leaving the impeller is given in Eq. (21) [16],

$$V'_2 = \sqrt{V_{r2}^2 + V_{\theta 2}^2} = 14.6259\,\text{m/s}. \quad (21)$$

2.5 Design of vanes

There are two methods of laying out the vane shape. They are tangent arcs and polar coordinates. In this study, tangent arcs method is used. The radial components V_{r1} and V_{r2} of absolute velocity at the inlet and outlet are 5.27w76 and 4.2221 m/sec these are plotted against corresponding radii of 42 mm and 68.50 mm, respectively, and may be connected by straight line or smooth curve as shown in Fig. 5.

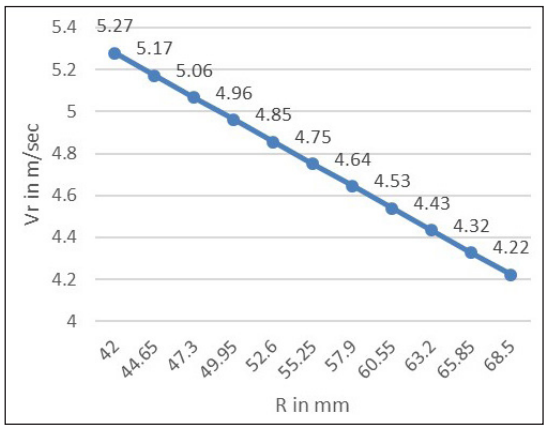

Fig. 5 *Vr* vs. *R*

The vane angles β_1 and β_2 at the inlet and outlet are 22° and 31°. Since, $w = Vr/\sin\beta$. The relative water velocity w will be 5.2776/sin22° = 14.0883 m/sec at inlet and 4.2221/sin31° = 8.1977 m/sec at outlet. These values may also be plotted against the radius and connected by straight line or smooth curve as shown in Fig. 6.

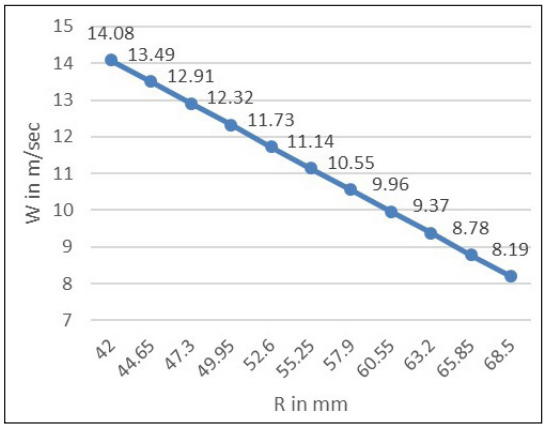

Fig. 6 W Vs. R

Intermediate values of *Vr* and *w* can be read from these curves. The corresponding values of vane angle β are computed from relationship, $\sin\beta = Vr/w$. The values of β thus found are plotted on the Fig. 7 and will be used in tangent arc method.

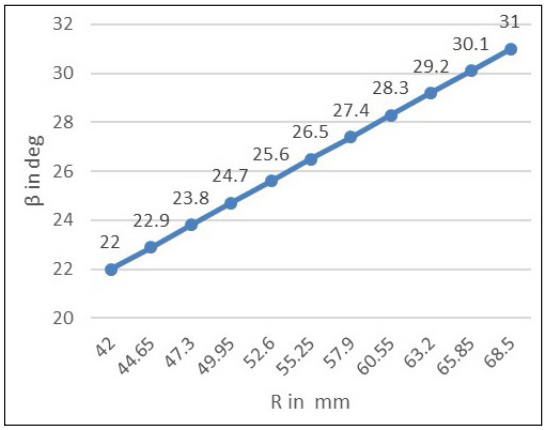

Fig. 7 β vs. *R*

Further, impeller is divided into number of concentric rings between R_1 and R_2. The radius (ρ) of the arc defining the vane shape between any two rings of radii R_b and R_a is given by Eq. (22). The radius is computed from Eq. (22) and presented in Table 1.

$$\rho = \frac{R_b^2 - R_a^2}{2\left(R_b\cos\beta_b - R_a\cos\beta_a\right)} \quad (22)$$

Fig. 8 represents vane profile drawn from Table 1. Any radial line OA from the Centre of rotation O to the radius R_1 is drawn. A line AB making an angle equal to $\beta_1 = 22^\circ$ with OA is then constructed. The Centre B for the first arc must lie on this line at a distance ρ of 5.24 cm from point A. A line drawn through

Table 1 Arc radius defining vane profile

Ring	Radius	R^2	**β**	cosβ	R**cosβ**	$R_b cos\beta_b - R_a cos\beta_a$	$R_b^2 - R_a^2$	ρ (mm)
1	42	1764	22	0.9272	38.9424			
2	44.65	1993.62	22.9	0.9212	41.1316	2.1892	229.623	52.45
3	47.3	2237.29	23.8	0.915	43.2795	2.1480	243.668	56.72
4	49.95	2495	24.7	0.9086	45.3846	2.1051	257.713	61.22
5	52.6	2766.76	25.6	0.9019	47.4399	2.0554	271.758	66.11
6	55.25	3052.56	26.5	0.895	49.4488	2.0089	285.803	71.14
7	57.9	3352.41	27.4	0.8879	51.4094	1.9607	299.848	76.47
8	60.55	3666.3	28.3	0.8805	53.3143	1.9049	313.893	82.40
9	63.2	3994.24	29.2	0.873	55.1736	1.8594	327.938	88.19
10	65.85	4336.22	30.1	0.8652	56.9734	1.7999	341.982	95.01
11	68.5	4692.25	31	0.8572	58.7182	1.7448	356.028	102.1

the inter-section of this arc with the ring b of radius 5.24 cm (point C) and point B must contain the Centre for the second arc F. This process is repeated until the outside ring at radius R_2 is reached. As a check on the accuracy of the work the angle ODE, where E is the Centre of last arc $\beta_2 = 31°$.

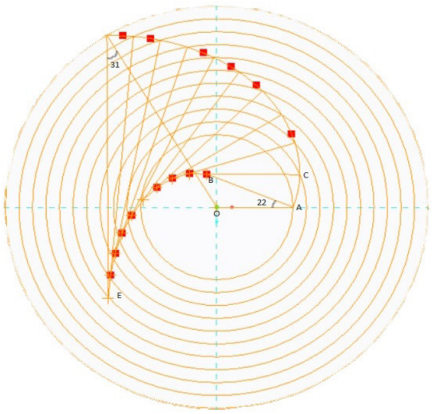

Fig. 8 Vane profile

3 Boundary conditions

Speed of 2970 RPM is given to centrifugal pump impeller domain. The working fluid through the pump is water at 27 °C. k-ε turbulence model with turbulence intensity of 5% is considered. Inlet Pressure of 0.6 kg/cm^2 and outlet mass flow rate of 14.51 kg/s (i.e., 0.01451 m^3/sec) are given as boundary conditions. Three-dimensional incompressible N-S equations are solved with Ansys-CFX Solver.

4 Procedure of CFD analysis

3D model of impeller and casing as shown in Fig. 9 and Fig. 10 are modelled in modelling software Creo 3.0 [17].

As hollow part of casing contains fluid, negative model of casing has to be created in order to create flow passage. In order to minimize losses, extra passage is added at inlet and outlet sections as shown by blue color in Fig. 11 [18].

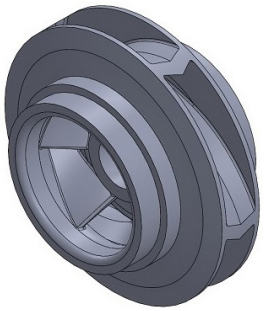

Fig. 9 Impeller

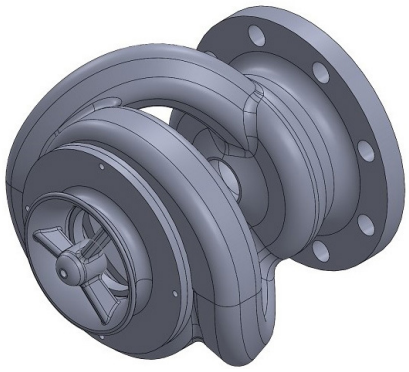

Fig. 10 Casing

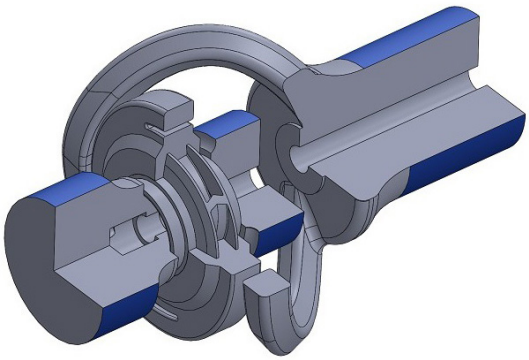

Fig. 11 Negative model of assembly

The model as shown in Fig. 11 is saved in neutral file format i.e. *.IGES format. Then model is imported into Ansys workbench mesh module for meshing. Fig. 12 represents cut view of mesh of model. Meshing Type: 3D, Type of Element: Tetrahedral. Minimum size of element is kept as 1.4637e-004 m.

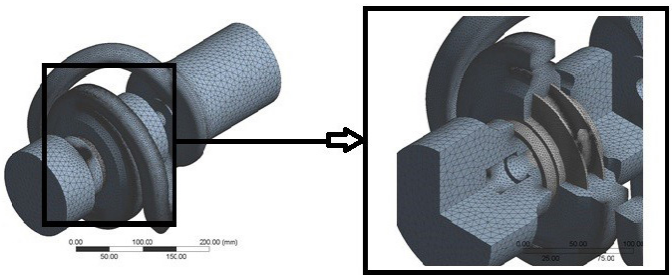

Fig. 12 Meshing of model

The grid convergence study was performed by developing three different meshes: with a coarse, medium, and fine grid for pump to predict the head developed. The number of nodes and the simulation time for the three cases simulated using the standard k-ε model are given in Table 2, it is very clear that CFD simulation time is highly dependent on the number of mesh nodes considered.

Table 2 Mesh size, CFD simulation time, and estimated Head for k-ε model

Mesh Resolution	Coarse Mesh (M1)	Medium mesh (M2)	Fine mesh (M3)
Number of nodes	763597	1069590	1626581
CFD simulation time	4 hrs 36min	6 hrs 06 min	9 hrs 50min
Estimated head (m)	23.9825	25.0623	25.1964

It is important to note that the mesh resolution plays a pivotal role in the final CFD results. The mesh nodes need to be small to resolve the boundary layer on the impeller surface. The highest head obtained from the mesh independent study is 25.0623 m for M2 from the k-ε model. M2 and M3 account for nearly 1% difference in the estimated head, but the final CFD simulation time required for convergence of the two meshes has a significant difference when the conventional mesh independency method is employed. M1 leads to the reasonable prediction of the head, whereas the head of M3 is slightly better than M2. Due to the slight difference medium mesh (M2) is best regarding computational costs.

After doing meshing of model definition of Inlets, Outlet, Wall, Impeller and hub done under named selection tab. Model then saved in *. CMDB format then imported it into ANSYS CFX Pre.

Defined Water Domain. With Domain Type: Fluid, Domain Fluid: Water, Domain motion: stationary. Defined new boundary inlet: - total pressure 0.6 kg/cm^2. Defined new boundary Outlet: - mass flow rate 14.51 kg/s, defined new boundary wall: - wall roughness smooth wall.

Defined domain 2. With Domain Type: immersed solid domain, Domain motion: Rotating, Domain RPM: 2970 RPM. Rotating about: Z Axis, Defined new boundary impeller: - boundary type wall.

Turbulence model is defined in this step as K-epsilon total energy turbulence model, where turbulence kinetic energy is defined as the variance of the fluctuations in velocity by notation K. ε represents the rate at which the velocity fluctuations dissipate i.e. the turbulence eddy dissipation, this puts two new variables into the system of equations. The continuity equation is as shown in Eq. (23) [19]:

$$\frac{\partial \rho}{\partial t} + \nabla \bullet \left(\rho U\right) = 0 \tag{23}$$

and the momentum equation is as given in Eq. (24),

$$\begin{aligned} &\frac{\partial \rho U}{\partial t} + \nabla \bullet \left(\rho U \otimes U\right) - \nabla \bullet \left(\mu ef\, f \nabla U\right) \\ &\quad = \nabla P' + \nabla \bullet \left(\mu ef\, f \nabla U\right) T + B \end{aligned} \tag{24}$$

Defined new expression to determine head developed, efficiency and input power of impeller,

For determining head, Eq. (25) can be used [20],

$$Head = \frac{P_{\text{outlet}} - P_{\text{inlet}}}{\rho * g} + \frac{V^2_{\text{outlet}} - V^2_{\text{inlet}}}{2 * g} \tag{25}$$

In Ansys Eq. (25) can be written in expression format as:

$$\begin{aligned} &(massFlowAve(TotalPressureinStnFrame)@outlet \\ &-massFlowAve(TotalPressureinStnFrame)@inlet) \\ &/(ave(Density)@outlet * g) \\ &+((massFlowAve((VelocityinStnFrame)^2)@outlet \\ &-massFlowAve((VelocityinStnFrame)^2)@inlet)/(2 * g)) \end{aligned}$$

For input power, formula is given in Eq. (26),

$$\text{Input power} = \text{Torque} * \text{angular velocity} \tag{26}$$

The value of torque about Z axis is considered as impeller is rotating about Z axis.

Input power equation can be written in expression language as,

$$I.P = \left(\text{torque\_z ()} @\text{impeller} * \text{angular velocity}\right)$$

Finally, efficiency can be calculated as given in Eq. (27),

$$\eta = \frac{\text{Output Power}}{\text{Input Power}} \tag{27}$$

Where,

$$\text{Output Power} = \text{Head} * \text{discharge} * \text{g} * \text{density}$$

Added head, input power and efficiency as monitor point to output control so as to monitor status of parameter during solution.

Solver control criteria is defined with, min number of iteration: 1, max. number iteration: - 1000, convergence criteria: RMS, residual target: 1e-4

Analysis is then initiated.

5 Results and discussion

From analysis at duty point i.e. at discharge of 0.01451 m^3/sec, following results are obtained Head developed: 25.0623 m, Pump input: 4.1 kw and Efficiency: 87.02 %.

5.1 Pressure contours

The pressure contours in Fig. 13 show a continuous rise in pressure from leading edge to trailing edge of the impeller due to the dynamic head developed by the pump impeller while rotating. The total pressure on discharge side of blade is more than suction side. The pressure difference from the discharge side to the suction side of the impeller blade is increasing from driving edge to trailing edge of the blade. The minimum value of the static pressure inside the impeller is located at the leading edge of the blades on the suction side.

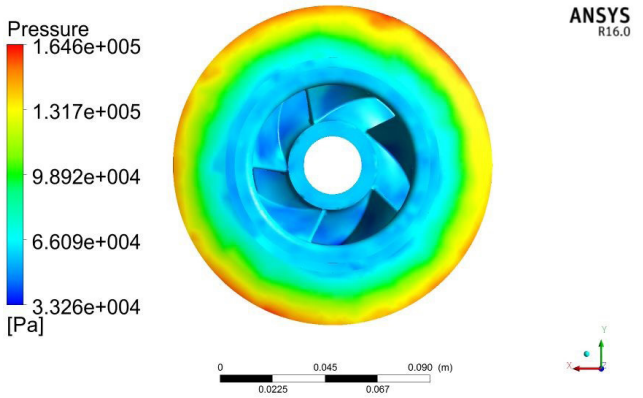

Fig. 13 Pressure distribution plot of impeller

Fig. 14 represents the pressure contours on original casing. From Fig. 14, it is clear that very uneven pressure distribution is developed in original casing which produced very low-pressure region near shaft of pump and high-pressure region near wall of casing. Max pressure observed in this case is $2.553*10^5$ Pa and min pressure $1.57*10^5$ Pa so the average becomes $2.0615*10^5$ Pa.

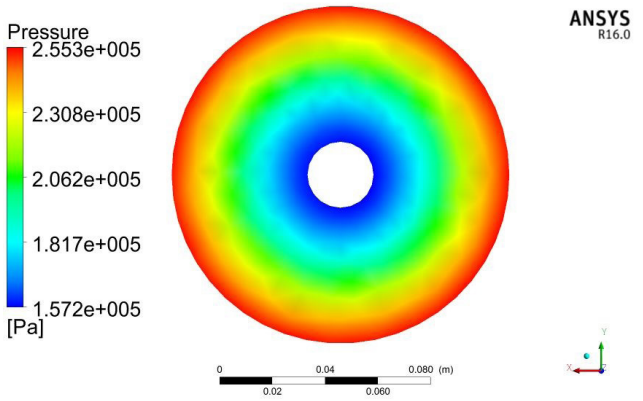

Fig. 14 Pressure distribution in original casing

5.2 Velocity contours

Fig. 15 shows the velocity contours on the impellers surface. It is clear from figure that velocity at outlet of impeller is 22.04 m/s which is nearly equal to velocity calculated from mathematical relations. Fig. 16 represents the velocity distribution in casing. Average velocity in outlet comes out to be 9.33804 m/sec and head developed comes out to be 25.0623 m. Fig. 17 denotes the vector plot of velocity inside the casing. From figure, it is clear that turbulence losses are very minimal in hydraulic portion of volute casing.

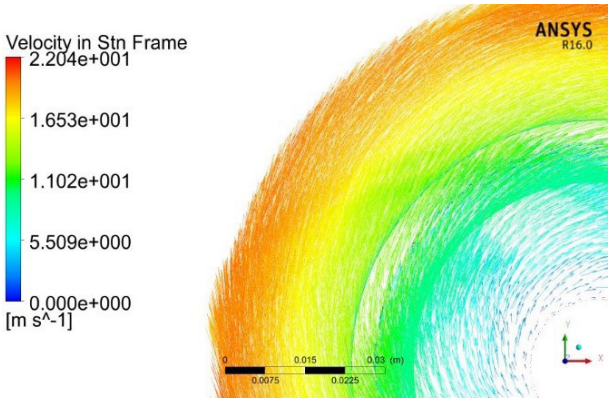

Fig. 15 Vector plot of velocity distribution in impeller

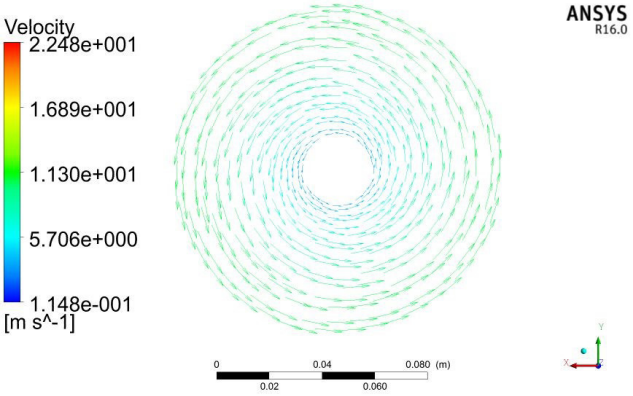

Fig. 16 Velocity Distribution in Original Casing

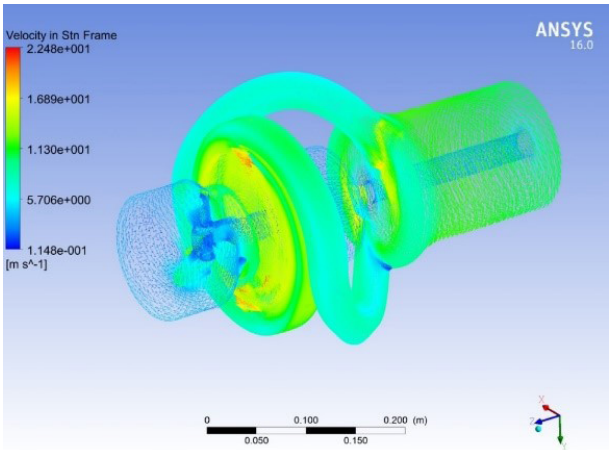

Fig. 17 Vector plot of velocity distribution in casing

Fig. 18 shows the streamline plot. From streamline plot it is clear that whirling of fluid takes place in the outlet portion of our casing. To make this flow laminar at outlet flow straightener can be induce, but it will create pressure loss thus head loss. Another way to make flow straight is by using two simple baffles, in this case the pressure loss in very minimal but effectiveness of this method is also less.

5.3 Characteristic curves

Fig. 19 shows the characteristic curve between discharge and head. Red line denotes the predicted curve while blue line denotes the curve obtained from CFD analysis. It shows that for this stage of pump the as discharge increases head decreases. As discharge rate increases the velocity of fluid also increases and due to increase in velocity pressure drop is observed. Thus, head reduces while discharge increases. According to analytical calcinations, head developed by impeller has to be 22 m. But, from analysis at duty point i.e. at discharge of 52 m^3/hr, head developed by pump comes out to be 25.063 m.

Fig. 20 shows the characteristic curve between discharge and overall efficiency. It shows that overall efficiency for this stage of pump starts decreasing after 52 m^3/hr. Velocity of the fluid increases due to increase in discharge rate and this high velocity cause cavitation losses and recirculation inside the impeller. Thus, efficiency is decreasing while operating in high discharge rate.

Fig. 21 shows the characteristic curve between discharge and power rating. It is clear from the graph that the power required to drive the pump increases as discharge rate increases. May be the reason for the increase in power rating is the increased blade loading during the operation.

6 Validation of CFD results

Simulation results can be validated by comparison with the experimental data. In this work, CFD head and theoretical head rise are the parameters that can be used for verification. The theoretical head rise can be obtained from the calculation results. Then, the theoretical head rise compared with that obtained from CFD results.

In the present study, the experimental work was not carried on. But, results from a previous study reported in the literature show good agreement between the theoretical head and the CFD head rise. However, due to recirculation, agreement becomes worst at very low discharge. An example of the comparison obtained from is shown in Table 3.

Table 3 Validation data

Paper name	Head obtained from CFD Analysis (m)	Head obtained from analytical methods(m)
Maitelli et al. [12]	22	20
Ozgen and Walters [3]	72	71
Heo et al. [5]	68	65
Present	25.063	22

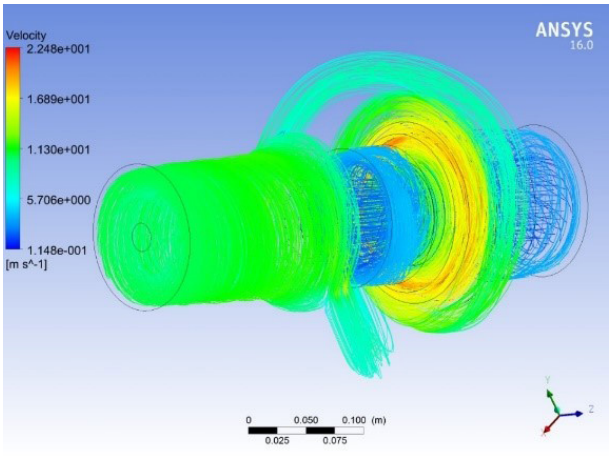

Fig. 18 Streamline distribution in Casing

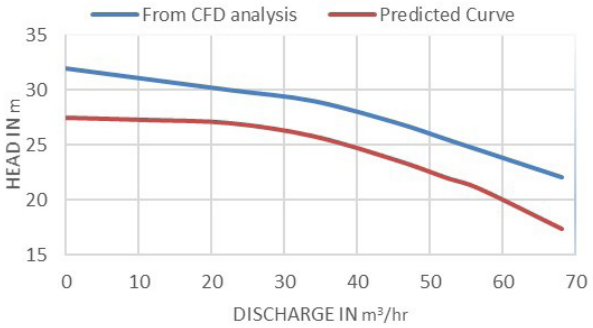

Fig. 19 Head vs. Discharge

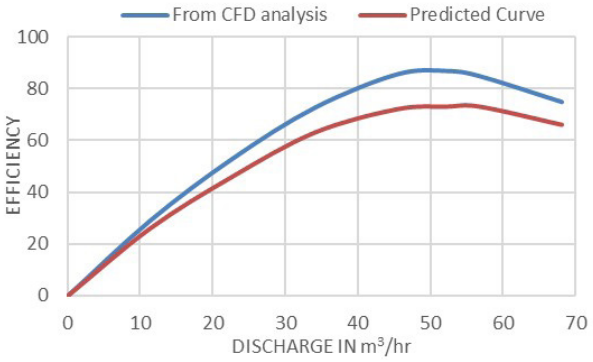

Fig. 20 Efficiency vs. Discharge

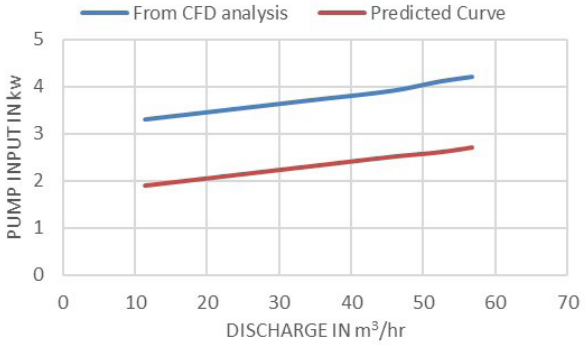

Fig. 21 Pump Input vs. Discharge

7 Conclusion

The ANSYS CFX has been used in this paper for the flow analysis of pump with double suction volute type. Modelling of impeller and volute geometry is done in software CREO 3.0 by assuming the required duty parameters as a case study are: Head = 22 m, Flow rate = 52.239 m^3/hr, RPM = 2970, Density = 1000 kg/ m^3, and the model prepared has been analysed in CFD tool CFX and its performance is analysed at different flow rates. It is found that the results obtained from design calculations and analyses are nearly similar. Thus, for general performance prediction this method is useful and less time consuming. In this way, design can be optimized to give reduced energy consumption, prolonged component life, lower head loss and better flexibility of the system, before the prototype is even built.

References

[1] Mehta, M. P., Patel, P. M. "Performance analysis and optimization of mixed flow pump." *International Journal of Emerging Trends in Engineering and Development*. 3(2), pp. 647–661. 2013. URL: http://rspublication.com/ijeted/may13/2.pdf

[2] Muttalli, R. S., Agrawal, S., Warudkar, S. "CFD simulation of centrifugal pump impeller using ANSYS-CFX." *Internationall Journal of Inovative Research in Science, Engineering and Technology*. 3(8), pp. 11–14. 2014. URL: http://www.rroij.com/open-access/cfd-simulation-of-centrifugal-pump-impellerusing-ansyscfx-.php?aid=48428

[3] Ozgen, O., Walters, K. "Design improvements on mixed flow pumps by means of computational fluid dynamics." A thesis submitted to the graduate school of natural and applied science of middle east technical university, pp. 2–44. 2006. URL: http://etd.lib.metu.edu.tr/upload/2/12608093/index.pdf

[4] Manivannan, A. "Computational fluid dynamics analysis of a mixed flow pump impeller." *International Journal of Engineering, Science and Technology*. 2(6), pp. 200–206. 2010.

[5] Heo, M.-W., Ma, S.-B., Skim, H.-S., Kim, K.-Y. "High-efficiency design optimization of a centrifugal pump." *Journal of Mechanical Science and Technology*. 30(9), pp. 3917-3927. https://doi.org/10.1007/s12206-016-0803-4

[6] Kim, J.-H., Lee, H.-C., Kim, J.-H., Kim, S., Yoon, J.-Y., Choi, Y.-S. "Design techniques to improve the performance of a centrifugal pump using CFD." *Journal of Mechanical Science and Technology*. 29(1), pp. 215-225. 2015. https://doi.org/10.1007/s12206-014-1228-6

[7] Sekino, Y., Watanabe, H. "Design optimization of double-suction volute pumps." *World Pumps*. 2016(5), pp. 32-35. 2016. https://doi.org/10.1016/S0262-1762(16)30101-8

[8] Rajendran, S., Purushothaman, K. "Analysis of a centrifugal pump impeller using ANSYS-CFX." *International Journal of Engineering, Research and Technology*. 1(3), pp. 01-06. 2012.

[9] Damor, J. J., Patel, D. S., Thakkar, K. H., Brahmbhatt, P. K. "Experimental and CFD analysis of centrifugal pump impeller- A case study." *International Journal of Engineering, Research and Technology*. 2(6), 2013.

[10] Patel, J. A., Patel, B. B. "Design and flow through CFD analysis of enclosed impeller." *International Journal of Engineering, Research and Technology*. 3(7), pp. 1367–1373. 2014.

[11] Zhou, W., Zhao, Z., Lee, T. S., Winoto, S. H. "Investigation of flow through centrifugal pump impellers using computational fluid dynamics." *International Journal of Rotating Machinery*. 9(1), pp. 49-61. 2003. https://doi.org/10.1155/S1023621X0300006X

[12] Maitelli, C. W. S. de P., Bezerra, V. M. de F., da Mata, W. "Simulation of flow in a centrifugal pump of ESP systems using computational fluid dynamics." *Brazilian Journal Petroleum And Gas, (ABPG)*. 4(1), pp. 001–009. 2010. URL: http://www.portalabpg.org.br/bjpg/index.php/bjpg/article/view/107/114

[13] Ajith, M. S., Jeoju, M. I. "Design and analysis of centrifugal pump impeller using ansys fluent." *International Journal of Science, Engineering and Technological Research (IJSETR)*. 4(10), pp. 3640–3643. 2015. URL: http://ijsetr.org/wp-content/uploads/2015/10/IJSETR-VOL-4-ISSUE-10-3640-3643.pdf

[14] Kaul, R. "CFD analysis of centrifugal pump's impeller of various designs and comparison of numerical results for various models." *International Journal of Currrent Engineering and Technological (IJCET)*. 1(4), pp. 192–196. 2016. URL: http://inpressco.com/wp-content/uploads/2016/03/Paper40192-196.pdf

[15] Nigussie, T., Dribssa, E. "Design and CFD Analysis of Centrifugal Pump." *International Journal of Engineering Research and General Science*. 3(3), pp. 668–677. 2015. URL: http://oaji.net/articles/2015/786-1436112770.pdf

[16] Church, A. H. "Design and optimization." In: *Centrifugal pumps and blowers*. (pp. 111–141.) 1st edition, Metropolitan Book Co. Pvt. Ltd., 1950.

[17] CREO Parametric Toolkit 3.0, *User's Guide, Datecode*, M110, PTC univeristy, pp. 79-214.

[18] ANSYS CFX Reference Guide, *ANSYS CFX Reference Guide, Release 16.0*, ANSYS, Inc., Jan 2016. pp. 4-120. https://www.scribd.com/doc/316668483/ANSYS-Fluent-Theory-Guide-pdf

[19] Singh, R. R., Nataraj, M. "Design and analysis of pump impeller using SWFS." *World Journal of Modelling and Simulation*. 10(2), pp. 152–160. 2014. URL: http://www.wjms.org.uk/wjmsvol10no02paper08.pdf

[20] Thin, K. C., Khaing, M. M., Aye, K. M. "Design and performance analysis of centrifugal pump." *World Academy of Science, Engineering, and Technology*. 46, pp. 422-429. 2008. URL: https://pdfs.semanticscholar.org/e351/0bae5253c090888ac43368b1a136c4b1d2b4.pdf